Hyperfine Interact (2018) 239:23
https://doi.org/10.1007/s10751-017-1477-8

Mössbauer spectroscopy $BaSrNi_xCo_{2-x}Fe_{12}O_{22}$ hexaferrite prepared by sol-gel method

A.-F. Lehlooh[1] · E. A. Al Rasheed[2] · M. R. Said[1] · A. Y. Hammoudeh[3] · I. Bsoul[4] · S. H. Mahmood[5]

Abstract A system of Y-type Ba-hexaferrite ($BaSrNi_xCo_{2-x}Fe_{12}O_{22}$ with $x = 0.0 - 2.0$) has been prepared from precursor powders synthesized by sol-gel auto-combustion method. The prepared system was investigated by XRD and Mössbauer spectroscopy (MS). The XRD patterns show the formation of the Y-type phase at a sintering temperature of 1100 °C. The Mössbauer spectra show pure magnetic splitting. The variations of the relative intensities of the magnetic components of the spectrum were consistent with the substitution of Nickel ions at octahedral sites. The hyperfine fields do not change appreciably with Ni substitution, due to the fact that replacement of magnetic Co^{2+} ions by Ni^{2+} ions or Fe^{3+} ions does not change the magnetizations of the sublattices appreciably, and consequently, does not affect the strength of the antiferromagnetic coupling between these sublattices appreciably.

Keywords Mössbauer spectroscopy · X-ray diffraction · Hyperfine interactions · Y-type hexaferrites · Sol-gel method

This article is part of the Topical Collection on *Proceedings of the International Conference on the Applications of the Mössbauer Effect (ICAME 2017), Saint-Petersburg, Russia, 3–8 September 2017*
Edited by Valentin Semenov

✉ A.-F. Lehlooh
aflehlooh@yu.edu.jo; alehlooh@yahoo.com

[1] Physics Department, Yarmouk University, Irbid, Jordan

[2] Physics Department, Umm Al-Qura University, Mecca, Saudi Arabia

[3] Chemistry Department, Yarmouk University, Irbid, Jordan

[4] Physics Department, Al al-Bayt University, Mafraq, Jordan

[5] Physics Department, The University of Jordan, Amman, Jordan

Published online: 19 March 2018

1 Introduction

Ferrites have continued to attract attention over the years, as they are relatively inexpensive, stable and have a wide range of technological applications including transformer cores, high quality filters, high and very high frequency circuits and operating devices [1–4]. The physical properties of ferrites can be controlled by the preparation conditions, chemical composition, sintering temperature, and type and amount of substitution [5–7]. Hexaferrites form an important group of ferrites known to have hard magnetic properties. According to their structure, hexaferrites have been classified into six main classes: M-type ($AFe_{12}O_{19}$), X-type ($A_2M_2Fe_{28}O_{46}$), W-type ($AM_2Fe_{16}O_{27}$), Y-type ($A_2M_2Fe_{12}O_{22}$), Z-type ($A_3M_2Fe_{24}O_{41}$), and U-type ($Ba_4M_2Fe_{36}O_{60}$), where A is an alkaline-earth ion, and M is a divalent metal ion [8].

Y-type hexagonal ferrite is an interesting material for microwave applications, due to its favorable properties with high cut-off frequencies, high and tunable initial permeability in hyper frequency range [3, 9, 10]. Also, Y-type hexaferrites have demonstrated potential for magnetoelectric applications [11, 12]. In addition, the use of ferrites in some applications such as multilayer ferrite inductors operating in the high frequency range, require lowering the synthesis temperature of the ferrite, and serious attempts have been made in this direction [13–15].

In hexagonal ferrites, the unit cell consists of spinel (S) blocks that alternate along the c-axis with hexagonal layers of two types: T (antiferromagnetic) and R (ferrimagnetic) blocks [5]. Specifically, the unit cell of Y-type consists of alternating S and T blocks according to the stacking sequence (ST) (ST)′ (ST)″ where the primes indicate rotation of the blocks by 120° around the c-axis. The Y-type hexagonal ferrite structure is rhombohedral with space group (R3m), and lattice parameters: $a = 5.9$ Å and $c = 43.5$ Å [16]. The M metal ions and Fe ions are distributed among six different interstitial sites having octahedral or tetrahedral coordinations with the large O^{2-} ions, as illustrated by Table 1 [17]. In all, 12 sites are tetrahedral and 30 are octahedral in this structure. It is worth noting that inside the T block, three octahedral ions, belonging to $6c_{VI}$ and $3b_{VI}$ sublattices, lie on a vertical threefold axis, the central $3b_{VI}$ ion sharing two faces of its coordination figure with the adjacent $6c_{VI}$ ions [18].

Recent studies on Co-Zn-Cu modified Y-Type hexaferrite had reported excellent magnetic properties of these systems in the super high frequency range compared to Ni-Cu-Zn cubic ferrites [19, 20]. Our recent MS study on $Ba_2Co_{2-x}Zn_xFe_{12}O_{22}$ showed that Co ions occupy octahedral sites in the T block and Zn ions occupy the two spin down tetrahedral sites of the S and T blocks [21]. It also showed that Zn substitution resulted in weakening the superexchange coupling between the various sublattices.

This work is concerned with synthesizing $BaSrCo_{2-x}Zn_xFe_{12}O_{22}$ hexaferrite using sol-gel auto-combustion method, and characterizing it by XRD and MS to obtain information about the phase formation and the cationic distribution among the various sublattices, which influence the properties of the ferrite.

2 Experimental procedure

A series of ferrite samples of $BaSrNi_xCo_{2-x}Fe_{12}O_{22}$ with x = 0.0, 0.5, 1.0 and 2.0 were prepared by using a citrate sol-gel auto combustion method [12]. The preparation of the solutions was carried out by weighing the proper amounts of $Fe(NO_3)_3.9H_2O$, $Sr(NO_3)_2$, $Ba(NO_3)_2$, $Co(NO_3).6H_2O$, $Ni(NO_3)_2.6H_2O$ and dissolving each in Bi-distilled water under agitation until total dissolution of solids. The solutions were added together,

Table 1 Metallic sublattices of Y structures and their properties

Sublattices	Coordination	Block	Number of ions per unit cell	Spin
$6c_{IV}$	Tetra	S	6	Down
$3a_{VI}$	Octa	S	3	Up
$18h_{VI}$	Octa	S-T	18	Up
$6c_{VI}$	Octa	T	6	Down
$6c_{IV*}$	Tetra	T	6	Down
$3b_{VI}$	Octa	T	3	Up

yielding a completely homogenous transparent solution within few seconds. After that citric acid aqueous solution was added at 80 °C to chelate Ba^{2+} Sr^{2+} and Fe^{3+} in the solution. The mixed solution was then neutralized to pH 7 by adding ammonia. The neutralized solutions were slowly evaporated until a highly viscous residue was formed. The dried gel was burned in a self-propagating combustion manner to form a loose powder. The burnt powders were first preheated at 450 °C for 1 h. Finally, the powders were calcined in air at 1100 °C for 4 h with a heating rate of 10 °C /min to obtain Y-type Barium-Strontium hexaferrite phase.

Mössbauer spectra were collected over 512 channels using a standard constant acceleration Mössbauer spectrometer with ^{57}Co/Cr source. Mössbauer spectra were analyzed using standard fitting routines to obtain the hyperfine interactions. The XRD Patterns were recorded using $(\theta - 2\theta)$ diffractometer with Cu-K_α radiation with ($\lambda = 1.54$ Å).

3 Results and discussion

3.1 XRD measurements

XRD patterns of the samples with $x = 0.0$, 0.5, 1.0 and 2.0 are shown in Fig. 1. Rietveld refinement of all patterns was performed using FullProf software to examine phase purity of the samples and obtain the refined cell parameters for the crystallographic structure. Rietveld analysis revealed that all investigated samples are single-phase consistent with the $Ba_2Co_2Fe_{12}O_{22}$Y-type ferrite standard (JCPDS 00-044-0207), and the refined cell parameters are listed in Table 2. The relatively low values of χ^2 indicates reliable fittings. The data in Table 2 indicated that both a and c lattice parameters for all substituted samples decreased with respect to the un- substituted sample which could be attributed to the smaller ionic radius of Ni^{2+} (0.700 Å) relative to Co^{2+} (0.735 Å).

The particle size of the powders was calculated using the famous Scherrer's equation: $D = 0.94\lambda/\beta\cos\theta$, where λ is the wavelength of the radiation, β is the peak width at half height (in radians) and θ is the peak position [22]. The average crystallite size for each sample was calculated from several peaks and the results are listed in Table 2.

3.2 Mössbauer spectroscopy

Mössbauer spectra for all samples (Fig. 2) showed broadened magnetic splitting consistent with different magnetic components. Since the metallic ions reside in six sites as shown in Table 1, the Mössbauer spectra should be fitted by six magnetic sextets. However, the relative intensities of these sextets could not be associated easily with the relative occupation

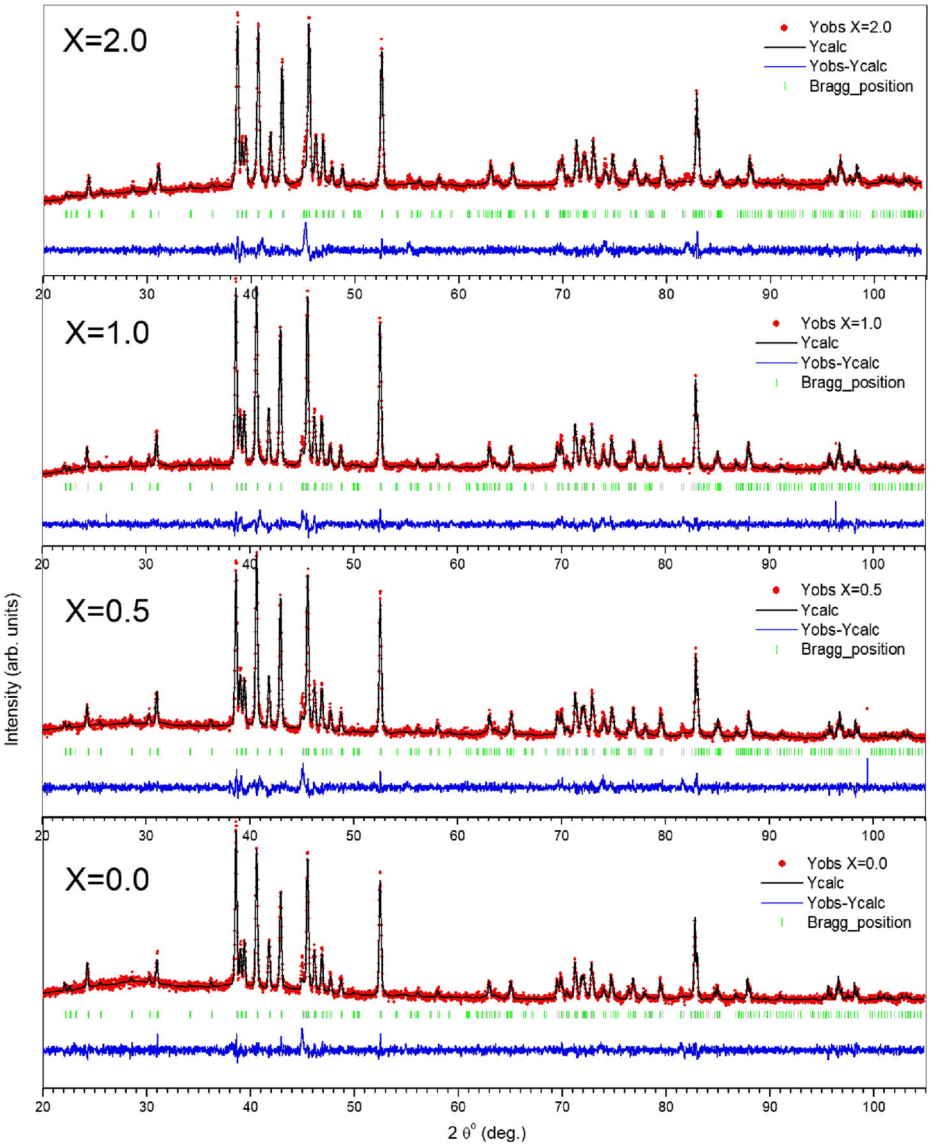

Fig. 1 Rietveld refinement of XRD patterns for the samples with $x = 0.0, 0.5, 1.0, 2.0$

Table 2 The lattice parameters derived from Rietveld refinement fitting of the XRD patterns and the crystallite size using Scherrer's formula

x	χ^2	a (Å)	c (Å)	V (Å)^3	ρ (g/cm^3)	D(nm)
0.0	1.38	5.858(2)	43.472(7)	1292.0(5)	5.25(5)	69.(3)
0.5	1.62	5.850(6)	43.424(1)	1287.2(4)	5.27(4)	65.(9)
1.0	1.51	5.851(5)	43.434(4)	1287.9(6)	5.27(1)	67.(8)
2.0	1.57	5.850(7)	43.393(1)	1286.3(9)	5.27(7)	58.(5)

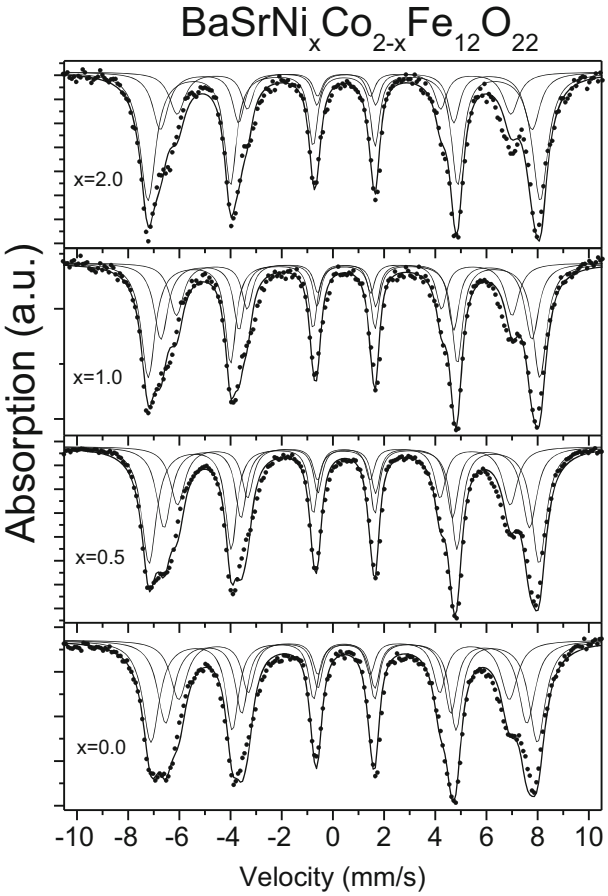

Fig. 2 Room temperature Mössbauer spectra of the samples $BaSrNi_xCo_{2-x}Fe_{12}O_{22}$ ($x = 0.0$, 0.5, 1.0 and 2.0)

of Fe ions at the corresponding sites. Hence, the room temperature spectra were fitted each with three magnetic sextets [17], and the fitting parameters are shown in Table 3.

The Mössbauer spectrum of $BaSrCo_2Fe_{12}O_{22}$ ($x = 0.0$) consists of three sub-spectra. The high field component (I) with $B_{hf} = 47.3$ T and relative intensity of 42% is associated with Fe^{3+} ions at the octahedral ($18h_{VI} + 3b_{VI}$) sites, the middle component (II) with $B_{hf} = 44.2$ T and relative intensity of 33% is associated with ($6c_{VI} + 6c^*_{IV}$) sites, and the low field component (III) with $B_{hf} = 40.4$ T and relative intensity of 25% is associated with ($3a_{VI} + 6c_{IV}$) sites. The values of the hyperfine parameters for this sample are listed in Table 3.

The maximum capacity of the ($18h_{VI} + 3b_{VI}$) sites is 7 metallic ions per formula unit, whereas the intensity of 42% for the corresponding component (I) suggests that these sites are occupied by only 5 Fe^{3+} ions out of the 12 per formula unit. This indicates that these sites are occupied by the 2 Co^{2+} ions, in addition to the 5 Fe^{3+} ions. This site preference for Co^{2+} ions is further confirmed by the 33% relative intensity for component (II), which is consistent with the maximum capacity of 4 ions for the ($6c_{VI} + 6c^*_{IV}$) sites, suggesting that these two sublattices are completely occupied by Fe^{3+} ions. Also, the maximum capacity of

Table 3 Room temperature Mössbauer parameters of $BaSrNi_xCo_{2-x}Fe_{12}O_{22}$ (x =0.0, 0.5, 1.0 and 2.0). Hyperfine field: B_{hf}(T), Relative Intensity: Int.(%), Center Shift: *CS* (mm/s), and Width: *W*(mm/s) of the spectral components

Mössbauer parameters	$x = 0.0$	$x = 0.5$	$x = 1.0$	$x = 2.0$
B_{hf} (I) (±0.5)	47.3	47.7	47.9	48.0
B_{hf} (II) (±0.5)	44.2	44.7	45.4	45.5
B_{hf} (III) (±0.5)	40.4	40.7	41.1	40.8
Int. (I) (±1)	42	45	47	57
Int. (II) (±1)	33	32	31	25
Int. (III) (±1)	25	23	22	18
CS (I) (±0.01)	0.44	0.43	0.43	0.43
CS (II) (±0.01)	0.52	0.52	0.52	0.52
CS (III) (±0.01)	0.43	0.44	0.44	0.43
W (I) (±0.02)	0.78	0.65	0.65	0.73
W (II) (±0.02)	0.59	0.50	0.50	0.56
W (III) (±0.02)	0.45	0.38	0.38	0.43

the ($3a_{VI}$+ $6c_{IV}$) sites is 3 ions, and thus the 25% intensity for the corresponding component (III) suggests that these two sublattices are completely occupied by Fe^{3+} ions.

Mössbauer spectrum of the sample with $x = 0.5$ was also fitted with three magnetic sextet components, and the values of the corresponding hyperfine parameters are listed in Table 3. The relative intensity of 45% for component (I) suggest that the corresponding $18h_{VI}$+ $3b_{VI}$ sublattices are occupied by 5.4 Fe^{3+} ions. As Ni^{2+} ions were reported to have preference for octahedral sites [18], the relative intensities for the three components suggest that Ni^{2+} ions are mainly distributed at $6c_{VI}$, $3a_{VI}$, with a small fraction (0.1) occupying the ($18h_{VI}$+ $3b_{VI}$) octahedral sites. This replacement results in the observed decrease of the relative intensities for the second and third components down to 32% and 23%, respectively, and the consequent increase in the relative intensity up to 45% for component (I) as a result of Fe^{3+} ions replacing the removed Co^{2+} from the ($18h_{VI}$+ $3b_{VI}$) sites. Analysis of the intensity of the three components at this level of Ni substitution indicates that 0.24 Ni^{2+} ions occupy the $3a_{VI}$ sites, 0.16 Ni^{2+} ions occupy the $6c_{VI}$ sites, while 0.10 Ni^{2+} ions occupy the ($18h_{VI}$+ $3b_{VI}$) sites.

The relative intensities of the three components for the sample with $x = 1.0$ confirm the preferential substitution of Ni^{2+} ions for Fe^{3+} ions at octahedral sites. Analysis of the relative intensities is consistent with the substitution of 0.36 Ni^{2+} ions at $3a_{VI}$ sites, 0.28 Ni^{2+} ions at $6c_{VI}$ sites, and 0.36 Ni^{2+} ions at ($18h_{VI}$+ $3b_{VI}$) sites. Thus, the substitution of Ni^{2+} ions is almost randomly distributed between the three preferred octahedral sites at this level of substitution.

Mössbauer spectrum of the sample with $x = 2.0$ is fitted with three magnetic sextet components having the hyperfine parameters listed in Table 3. The intensity of 57% for the first component suggests that the ($18h_{VI}$+ $3b_{VI}$) sites are occupied by 6.84 Fe^{3+} ions out of the 12 ions per formula unit. This suggests that 0.16 Ni^{2+} ions occupy these sites. The majority of Ni ions substitute Fe ions at $3a_{VI}$ and $6c_{VI}$ sites. In this $BaSrNi_2$-Y hexaferrite sample, Ni^{2+} ions demonstrate preference for $6c_{VI}$ sites, where 0.84 Ni^{2+} ions occupy the $3a_{VI}$ sites, and 1.0 Ni^{2+} ions occupy the $6c_{VI}$ sites.

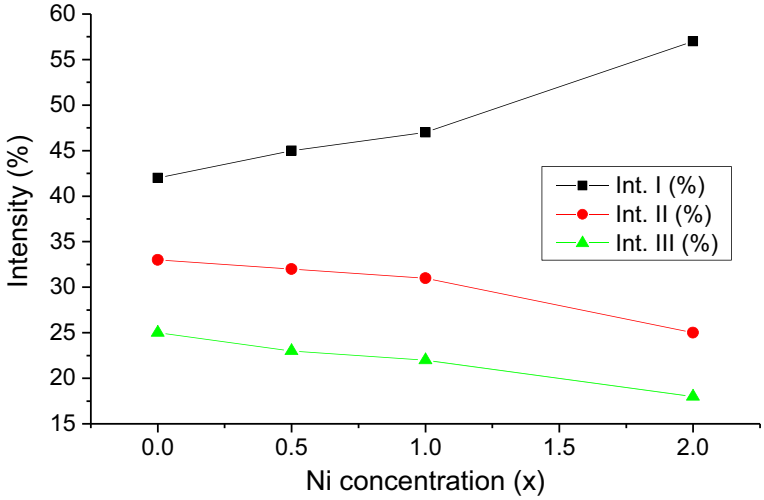

Fig. 3 The relative intensity of the three fitted spectral components (I, II and III) of $BaSrNi_xCo_{2-x}Fe_{12}O_{22}$ (x = 0.0, 0.5, 1.0 and 2.0)

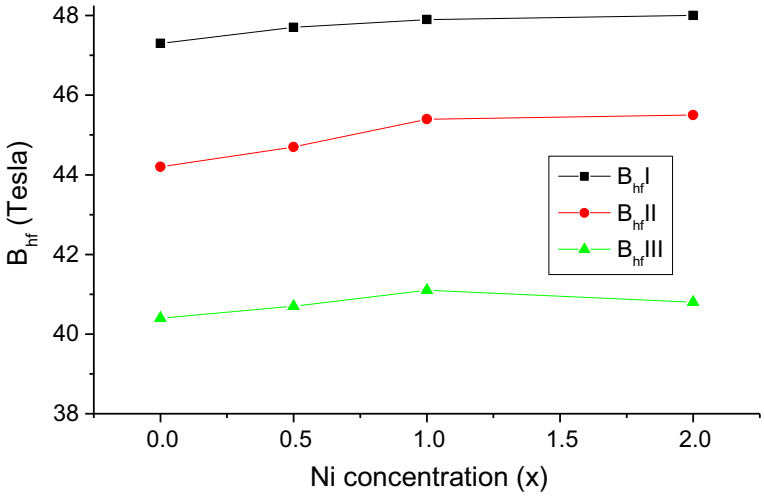

Fig. 4 The hyperfine fields B_{hf} of the three fitted spectral components (I, II and III) of $BaSrNi_xCo_{2-x}Fe_{12}O_{22}$ (x = 0.0, 0.5, 1.0 and 2.0)

The variations of the relative intensities of the magnetic components of the spectrum are shown in Fig. 3. It shows a decrease in the relative intensity of the second and third components, and an increase in the relative intensity of the first component, which indicates that nickel ions substitute iron ions at octahedral sites. The above analysis indicates that Ni^{2+} ions are almost randomly distributed between the octahedral sites at relatively low concentrations (x = 0.5 and 1.0), and demonstrate preference $3a_{VI}$ and $6c_{VI}$ octahedral sites at higher concentration (x = 2.0).

Figure 4 shows the hyperfine fields of the three components versus Ni substitution. The hyperfine field does not change appreciably with Ni substitution. This is due to the fact that

replacement of magnetic Co^{2+} ions by Ni^{2+} ions or Fe^{3+} ions does not change the magnetizations of the sublattices appreciably, and consequently the antiferromagnetic coupling between these sublattices is not weakened appreciably by the substitution.

4 Conclusions

The XRD patterns show single-phase consistent with the $Ba_2Co_2Fe_{12}O_{22}$ Y-type ferrite standard (JCPDS 00-044-0207) for all samples. Mössbauer spectra for the samples are consistent with Co^{2+} ions occupying $3b_{VI}$ and $18h_{VI}$ octahedral sites. The variations of the relative intensities of the magnetic components of the spectra (the increase of the first component and decrease of the second and third components) lead to the conclusion that Ni^{+} ions do not exhibit preference for a particular octahedral site at low Ni concentrations ($x = 0.5$ and 1.0). However, the distribution of Ni^{2+} ions exhibited preference for $3a_{VI}$ and $6c_{VI}$ sites at higher Ni^{2+} concentrations. The hyperfine field does not change appreciably with Ni substitution, indicating that the replacement of magnetic Co^{2+} ions by Ni^{2+} ions or Fe^{3+} ions does not change the magnetizations of the sublattices appreciably, and consequently the antiferromagnetic coupling between these sublattices is not weakened appreciably by the substitution.

Acknowledgments This work has been supported by a grant from Science Research support Fund (SRF) in Jordan and the Deanship of Scientific Research and Graduate Studies at Yarmouk University.

References

1. Pullar, R.C.: Hexagonal ferrites: a review of the synthesis, properties and applications of hexaferrite ceramics. Prog. Mater. Sci. **57**, 1191–1334 (2012)
2. Mahmood, S.H.: Permanent magnet applications. In: Mahmood, S.H., Abu-Aljarayesh, I. (eds.) Hexaferrite Permanent Magnetic Materials, pp. 153–165. Materials Research Forum LLC, Millersville (2016)
3. Bai, Y., Zhou, J., Gui, Z., Yue, Z., Li, L.: Complex Y-type hexagonal ferrites: an ideal material for high-frequency chip magnetic components. J. Magn. Magn. Mater. **264**, 44–49 (2003)
4. Harris, V.G., Geiler, A., Chen, Y., Yoon, S.D., Wu, M., Yang, A., Chen, Z., He, P., Parimi, P.V., Zuo, X.: Recent advances in processing and applications of microwave ferrites. J. Magn. Magn. Mater. **321**, 2035–2047 (2009)
5. Mahmood, S.H.: Properties and synthesis of hexaferrites. In: Mahmood, S.H., Abu-Aljarayesh, I. (eds.) Hexaferrite Permanent Magnetic Materials, pp. 74–110. Materials Research Forum LLC, Millersville (2016)
6. Mahmood, S.H., Zaqsaw, M.D., Mohsen, O.E., Awadallah, A., Bsoul, I., Awawdeh, M., Mohaidat, Q.I.: Modification of the magnetic properties of Co_2Y hexaferrites by divalent and trivalent metal substitutions. Solid State Phenom. **241**, 93–125 (2016)
7. Mahmood, S.H., Aloqaily, A.N., Maswadeh, Y., Awadallah, A., Bsoul, I., Awawdeh, M., Juwhari, H.: Effects of heat treatment on the phase evolution, structural, and magnetic properties of Mo-Zn doped M-type hexaferrites. Solid State Phenom. Trans. Tech. Publ. **232**, 65–92 (2015)
8. Chikazumi, S.: Physics of Ferromagnetism 2e, 2nd edn. Oxford University Press, Oxford (2009)
9. Chua, M.J., Yang, Z.H., Li, Z.W.: Structural and microwave attenuation characteristics of ZnCuY barium ferrites synthesized by a sol–gel auto combustion method. J. Magn. Magn. Mater. **368**, 19–24 (2014)
10. Murtaza, G., Ahmad, R., Hussain, T., Ayub, R., Ali, I., Khan, M.A., Akhtar, M.N.: Structural and magnetic properties of Nd–Mn substituted Y-type hexaferrites synthesized by microemulsion method. J. Alloys Compd. **602**, 122–129 (2014)
11. Khanduri, H., Dimri, M.C., Kooskora, H., Heinmaa, I., Viola, G., Ning, H., Reece, M., Krustok, J., Stern, R.: Structural, dielectric, magnetic, and nuclear magnetic resonance studies of multiferroic Y-type hexaferrites. J. Appl. Phys. **112**, 073903 (2012)

12. Koutzarova, T., Kolev, S., Nedkov, I., Krezhov, K., Kovacheva, D., Blagoev, B., Ghelev, C., Henrist, C., Cloots, R., Zaleski, A.: Magnetic properties of nanosized $Ba_2Mg_2Fe_{12}O_{22}$ powders obtained by auto-combustion. J. Supercond. Nov. Magn. **25**, 2631–2635 (2012)
13. Bierlich, S., Töpfer, J.: Zn-and Cu-substituted Co_2Y hexagonal ferrites: sintering behavior and permeability. J. Magn. Magn. Mater. **324**, 1804–1808 (2012)
14. Kračunovska, S., Töpfer, J.: Synthesis, sintering behavior and magnetic properties of Cu-substituted Co_2Z hexagonal ferrites. J. Mater. Sci.: Mater. Electron. **22**, 467–473 (2011)
15. Bai, Y., Zhang, W., Qiao, L., Zhou, J.: Low-fired Y-type hexagonal ferrite for hyper frequency applications. J. Adv. Ceram. **1**, 100–109 (2012)
16. Collomb, A., Muller, J., Fournier, T.: Magnesium location in the barium-magnesium-iron Y-type hexagonal ferrite. Mater. Res. Bull. **28**, 621–627 (1993)
17. Deriu, A., Licci, F., Rinaldi, S., Besagni, T.: Y-type hexagonal ferrites containing zinc, copper and cadmium: magnetic properties and cation distribution. J. Magn. Magn. Mater. **22**, 257–262 (1981)
18. Albanese, G.: Recent advances in hexagonal ferrites by the use of nuclear spectroscopic methods. J. Phys. Colloq. **38**, 85–94 (1977)
19. Bai, Y., Zhou, J., Gui, Z., Li, L., Qiao, L.: The physic properties of Bi–Zn codoped Y-type hexagonal ferrite. J. Alloys Compd. **450**, 412–416 (2008)
20. Bai, Y., Xu, F., Qiao, L., Zhou, J.: Effect of Mn doping on physical properties of Y-type hexagonal ferrite. J. Alloys Compd. **473**, 505–508 (2009)
21. Mahmood, S.H., Jaradat, F.S., Lehlooh, A.F., Hammoudeh, A.: Structural properties and hyperfine interactions in Co-Zn Y-type hexaferrites prepared by sol-gel method. Ceram. Int. **40**, 5231–5236 (2014)
22. Bsoul, I., Mahmood, S.H.: Structural and magnetic properties of $BaFe_{12-2x}Ti_xRu_xO_{19}$. J. Alloys Compd. **498**, 157–161 (2010)